

Spin fluctuations in an amorphous alloy

A. LeR. Dawson and D. H. Ryan

Department of Physics, McGill University, 3600 University St., Montreal, Quebec, Canada H3A 2T8

David V. Baxter

Department of Physics, Indiana University, 117 Swain Hall W., Bloomington, Indiana 47405

(Received 17 June 1996)

Enhancement of the effective electron mass by spin fluctuations (SF's) has been studied in $a\text{-Fe}_x\text{Zr}_{100-x}$ ($27\% \leq x \leq 39\%$) by low-temperature calorimetry. Previous magnetization measurements on paramagnetic $a\text{-Fe}_x\text{Zr}_{100-x}$ are also presented and analyzed to extract the ground-state susceptibility $\chi(T=0)$. The low spin fluctuation temperature of ~ 7 K and the stable amorphous structure make it possible to unambiguously distinguish between magnetic and nonmagnetic contributions to the electronic specific heat. The SF contribution to the specific heat shows a clear maximum around the critical composition for the onset of magnetic order ($x_c \sim 37\%$), with the mass enhancement parameter λ_{SF} reaching ~ 1 . Complete quenching of SF's by both temperature and an external magnetic field have been observed. As a result of its low characteristic temperature ($T_{\text{SF}} \sim 7$ K), $a\text{-Fe}_{36}\text{Zr}_{64}$ shows the clearest evidence to date of the effects of SF's on electronic properties. [S0163-1829(96)06541-1]

I. INTRODUCTION

Historically, an understanding of magnetism in solids has been approached from two perspectives, the local moment picture, developed for insulators and rare earth metals, and the itinerant moment picture which describes magnetized alkaline and noble metals. Determining which model applies to d -electron transition metals underlines a controversy that lasted 50 years.¹ While the ground-state properties of the iron group metals were finally demonstrated to be explainable within the itinerant model, mean-field Stoner theory proved unable to explain their finite-temperature properties. The failure of Stoner theory can be traced to its neglect of magnetization fluctuations, or spin fluctuations (SF's) as they are called in a metal. These nonpropagating excitations with a characteristic energy $k_B T_{\text{SF}}$ are now believed to determine all finite-temperature magnetic properties of transition metals, notably the critical temperature T_c ,²⁻⁴ particularly in weak itinerant ferromagnets. Measurement of static magnetic properties cannot unambiguously identify the presence of SF's⁵, as their characteristic behavior does not dominate over a wide enough temperature range for it to be unambiguously distinguished from other contributions. Consequently, experimental evidence for the existence of SF has come mainly from observations of SF scattering effects on electronic properties⁶⁻⁸ and from neutron scattering results.^{3,4,9}

The effects of SF's are most evident near T_c , and are especially clear in marginal magnetic systems where T_c approaches zero. In such cases, SF's may be studied at low temperatures where many other excitations are largely frozen out or have simple functional forms. Recent experimental studies have concentrated on the itinerant, weakly magnetic Ni_3Al system^{6,7} ($\text{Ni}_x\text{Al}_{100-x}$, $x \sim 75\%$) as the composition is varied slightly off stoichiometry. This allows the study of SF's as the strength of the magnetism is varied through the critical concentration for the onset of magnetic order. However, changing the composition also affects the atomic struc-

ture, turning a perfect ordered intermetallic crystal Ni_3Al into one containing an increasing number of defects as one moves further away from the stoichiometric ratio. The ideal system for the study of SF's would be an itinerant magnet in which one could vary only the strength of the magnetism while keeping the atomic structure constant.

We have found amorphous iron-zirconium ($a\text{-Fe}_x\text{Zr}_{100-x}$) to be such a system. On increasing the iron content through the critical composition, $x_c \sim 37\%$, this system undergoes a transition from a nearly ferromagnetic metal to a weak itinerant ferromagnet,^{10,11} while the atomic structure remains virtually unchanged. Earlier studies observed SF scattering in the low-temperature resistivity in this system.^{12,13} We report here the effects of SF scattering on the effective electron mass, studied by measuring the low-temperature specific heat at finely spaced composition intervals around $x_c \sim 37\%$ (shown in Fig. 1). The narrow temperature range over which SF effects dominate is used to advantage here, as it allows us to determine the "normal," i.e., SF-free, properties by measuring at temperatures high enough for SF effects to be absent, but low enough that the electronic specific heat is still substantial. We can then unambiguously determine the SF contributions at lower temperatures. The effects of an applied field are used first to rule out magnetic clustering, and then to obtain semiquantitative agreement with model predictions. We have observed the complete quenching of the SF contribution by both temperature and applied magnetic field in a metallic system.

II. MAGNETOMETRY RESULTS

The magnetization of five paramagnetic amorphous iron-zirconium ($a\text{-Fe}_x\text{Zr}_{100-x}$) samples was previously studied by Trudeau *et al.*¹¹ Following the work of Ref. 10, we reanalyze the data above 5 kOe in a manner more appropriate for exchange enhanced Pauli paramagnets (near ferromagnets) in

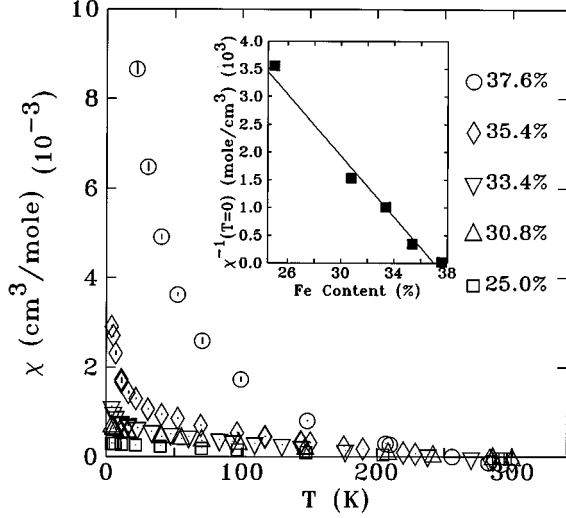


FIG. 1. The measured molar magnetic susceptibility $\chi(T)$ for five paramagnetic $a\text{-Fe}_x\text{Zr}_{100-x}$ samples. Inset: values of the ground-state inverse susceptibility $\chi^{-1}(T=0)$. The solid line is consistent with Stoner theory [Eq. (3)].

order to show that the behavior is consistent with the presence of spin fluctuations and to obtain parameters needed for the analysis of the calorimetry data presented below. A simple derivation is given of a high-temperature Curie-Weiss law resulting from spin fluctuations. This relation is then compared with the high-temperature data.

In a system with a small uniform magnetization M , the free energy may be approximated by a Ginzburg-Landau expansion.³ The result is that the applied magnetic field H and the magnetization M are related by

$$\frac{H}{M} = a + bM^2, \quad (1)$$

so that in an Arrott plot of H/M vs M^2 , the data should follow a straight line. In paramagnetic samples, both a and b are greater than zero and the straight lines cut the x axis at a point corresponding to the inverse magnetic susceptibility, $a \equiv \chi^{-1}$. The temperature dependence of the molar susceptibilities obtained in this way is shown in Fig. 1. Since we are concerned primarily with low-temperature behavior, we neglect contributions from the Van Vleck susceptibility of Zr ($\sim 1.2 \times 10^{-4}$ cm³/mol) and the Larmor diamagnetic contribution due to core electrons ($\sim -0.3 \times 10^{-4}$ cm³/mol),¹⁰ which are never more than 10% of our extrapolated values. We have also neglected the small Landau diamagnetic contribution [$-\frac{1}{3}\chi_P(T=0)$] of the conduction electrons to χ .

Stoner theory predicts that the susceptibility of a nearly ferromagnetic metal should be weakly quadratically dependent on temperature.^{14,15} Clearly, this is not a correct description of the rather strong temperature dependence in the measured susceptibility of $a\text{-Fe}_x\text{Zr}_{100-x}$ apparent in Fig. 1. Nonetheless, following previous work on nearly magnetic Ni₃Ga,¹⁶ we have used a parabola of the form: $\chi^{-1}(T) = \chi^{-1}(T=0) + [\text{const.}]T^2$, as an extrapolation scheme to obtain the values of $\chi^{-1}(T=0)$, the inverse ground-state susceptibility, displayed in the inset to Fig. 1.

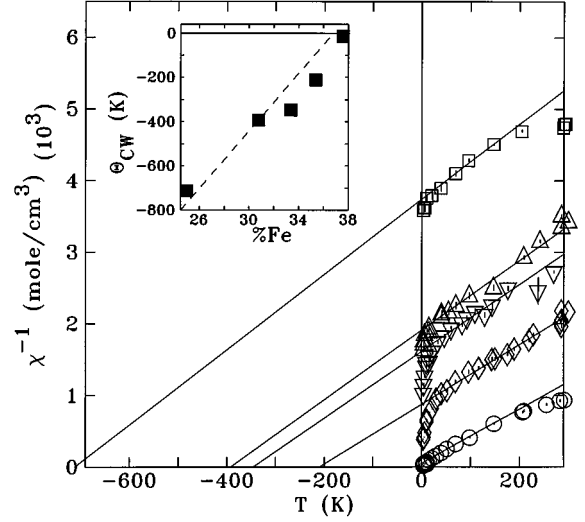


FIG. 2. Inverse molar susceptibility of $a\text{-Fe}_x\text{Zr}_{100-x}$. Straight solid lines are fits to a Curie-Weiss law [Eq. (4)] between 50 K and 200 K. Samples are indicated by the same symbols used in Fig. 1. The inset shows the values of Θ_{CW} determined from the straight lines.

These values are far larger than those expected for a simple metal ($\sim 10^{-6}$ cm³/mol) and we therefore conclude that the $a\text{-Fe}_x\text{Zr}_{100-x}$ samples are strongly exchange-enhanced paramagnets or near ferromagnets. In this case, Stoner theory predicts the relation

$$\chi = S\mu_B^2 N_0(\varepsilon_F), \quad (2)$$

where μ_B is the Bohr magneton, $S \equiv (1 - \bar{I})^{-1}$ is the Stoner enhancement factor, and $N_0(\varepsilon_F)$ is the bare densities of states at the Fermi level, ε_F . The inverse ground-state molar susceptibilities in Fig. 1 may be fitted with a linear function of iron content x , namely,

$$\chi^{-1}(T=0) = (2.76 \times 10^4 \text{ mol/cm}^3)(36.8\% - x)/100\%. \quad (3)$$

This line, shown in the inset to Fig. 1, suggests a critical concentration of $x_c \sim 37\%$ for the onset of ferromagnetism, where the susceptibility diverges. The $x = 37.6\%$ sample was omitted from the fit since this sample was calorimetrically determined to exhibit a magnetic ordering transition just below 4 K,¹⁷ an observation that is consistent with our estimated value of x_c . A linear relation is consistent with Stoner theory,^{5,14,15} assuming that $N_0(\varepsilon_F)$ varies linearly in Fe content. Equations (2) and (3), combined with calorimetric estimates of $N_0(\varepsilon_F)$, will be used to determine the Stoner factors of the calorimetry samples.

A Curie-Weiss analysis

$$\chi(T) = \frac{C_{\text{CW}}}{T - \Theta_{\text{CW}}} = \frac{p_{\text{eff}}^2 N_A}{3k_B(T - \Theta_{\text{CW}})} \quad (4)$$

of the high-temperature inverse susceptibility between 50 K and 200 K (Fig. 2) shows that all Θ_{CW} values are negative, rising towards zero with increasing Fe content, and vanishing at x_c (inset to Fig. 2). Negative Θ_{CW} values from high-temperature Curie-Weiss fits are typical of nearly ferromag-

netic metals such as Ni_3Ga .¹⁶ The fitted Curie-Weiss constants $C_{\text{CW}} \equiv \lim_{T \rightarrow \infty} (d\chi^{-1}/dT)^{-1}$ increase with Fe content from $0.19 \text{ K cm}^3/\text{mol}$ at $x=25.0\%$ to $0.26 \text{ K cm}^3/\text{mol}$ at $x=37.6\%$. C_{CW} can be used to calculate the effective high-temperature Curie moment, given by $p_{\text{eff}}^2 \equiv p_C(p_C + 2\mu_B)$. These range from $p_C = 0.58\mu_B$ to $0.76\mu_B$.

Although traditionally taken as a manifestation of local moments, a Curie-Weiss law may also be derived using the spin fluctuation models which apply to itinerant magnets.^{1,3} In the simplest theories^{2,18} SF's renormalize the Ginzburg-Landau coefficient, a in Eq. (1) (or equivalently the noninteracting susceptibility χ_0), by a small constant $\alpha(T)$. A simple way to visualize the origin of $\alpha(T)$ is as follows: A spin fluctuation saturates the magnetization in its immediate vicinity; this volume therefore cannot respond to an external field and so its apparent susceptibility is reduced. $\alpha(T)$ is then a sum over all SF's and represents the ‘‘magnetically dead’’ volume fraction of the sample. Alternatively, SF's, can be viewed as introducing an effective pressure,¹⁸ which renormalizes the Ginzburg-Landau coefficients. Either way, the renormalized susceptibility $\bar{\chi}_0(T)$ may be written as¹⁹

$$\bar{\chi}_0(T) = \frac{\chi_0(T)}{1 + \alpha(T)}.$$

In standard Weiss molecular field theory, the interacting susceptibility $\chi(T)$ is determined directly from the noninteracting susceptibility, now $\bar{\chi}_0(T)$, and a molecular field constant, λ :

$$\chi(T) = \frac{\bar{\chi}_0(T)}{1 - \lambda \bar{\chi}_0(T)} \approx \frac{\chi_P(T=0)}{1 - \bar{I} + \alpha(T)},$$

where we have neglected the temperature dependence of the Pauli susceptibility, in writing $\lambda \chi_0(T) \approx \lambda \chi_P(T=0) \equiv \bar{I}$. $\alpha(T)$ is expected to be proportional to the number of SF occupying each SF mode. This is in turn proportional to the Bose factor which, at high temperatures ($T \gg T_{\text{SF}}$), is simply T/T_{SF} . Writing $\alpha(T) = cT/T_{\text{SF}}$, we have

$$\chi(T) = \frac{T_{\text{SF}} \chi_P(T=0)/c}{T - T_{\text{SF}}(\bar{I} - 1)/c}. \quad (5)$$

This is the Curie-Weiss law with $\Theta_{\text{CW}} = T_{\text{SF}}(\bar{I} - 1)/c$. Notice that Θ_{CW} has the same sign as $\bar{I} - 1$: positive for weak ferromagnets, negative for near ferromagnets, and passing through zero at x_c . This behavior is clearly seen in the inset to Fig. 2. At low temperatures $T < T_{\text{SF}}$, the approximation leading to the Curie-Weiss law breaks down, since the SF modes are not all excited. $\chi(T=0)$ should, therefore, be larger than the value extrapolated from the Curie-Weiss law [Eq. (5)] and a plot of χ^{-1} vs T falls away from the Curie-Weiss line on approaching $T=0$ (Fig. 2).

The magnetization data show that the critical iron concentration for the development of magnetic order in this system is $x_c = 37\%$. $\chi(T=0)$ is far larger than expected for a simple metal and indicates the presence of strong exchange enhancement. The negative Curie-Weiss temperatures and the down-turns in the χ^{-1} vs T plots (Fig. 2) are fully consistent with SF models. All of these results lead us to expect a

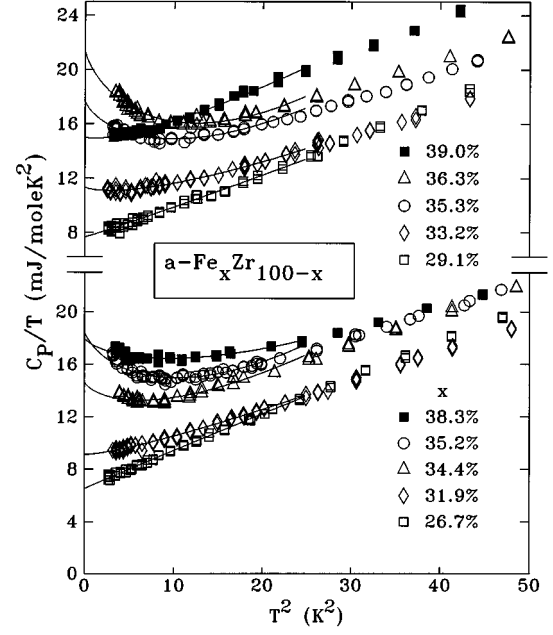


FIG. 3. Low-temperature specific heat of various $a\text{-Fe}_x\text{Zr}_{100-x}$ samples. Alloys with Fe concentrations greater than the critical concentration ($x_c \sim 37\%$) are plotted as solid symbols. The solid lines are fits to the Eq. (7) below 5 K. For clarity, samples have been plotted alternately in the top and bottom regions.

significant SF contribution to the specific heat, which should reach a maximum as T_c passes through zero at x_c .

III. CALORIMETRY RESULTS

The magnetocalorimetry studies were carried out on a series of paramagnetic and ferromagnetic $a\text{-Fe}_x\text{Zr}_{100-x}$ samples, whose compositions were determined by electron microprobe analysis. One of the calorimetry samples ($x = 37.6\%$) was taken from the susceptibility series. Sample preparation, characterization, and absolute calorimetry measurements have been described elsewhere.^{17,20} We note here only that the absolute accuracy of the calorimeter was determined to be $\pm 2\%$ by measuring the specific heat $C_p(T)$ of gold and copper standards.²¹ $C_p(T)$ values in a magnetic field were determined using a field-independent capacitance thermometer.

Figure 3 shows the molar specific heat $C_p(T)$ for several $a\text{-Fe}_x\text{Zr}_{100-x}$ samples between $\sim 2 \text{ K}$ and 7 K , plotted as C_p/T vs T^2 . For a normal metal, we expect

$$\frac{C_p(T)}{T} = \gamma + \beta T^2 \text{ for } T < \Theta_D/20, \quad (6)$$

where

$$\gamma = (1 + \lambda_{e-p}) \frac{1}{3} \pi^2 k_B^2 N_0(\epsilon_F) \equiv (1 + \lambda_{e-p}) \gamma_0$$

and

$$\beta = \frac{(1.944 \times 10^6 \text{ mJ/mol K})}{\Theta_D^3}.$$

The electron mass enhancement factor λ_{e-p} arises through the electron-phonon interaction and $N_0(\varepsilon_F)$ is the bare electron density of states at the Fermi energy ε_F . βT^3 is the standard low-temperature limiting form of the specific heat due to phonons with a Debye temperature Θ_D . Since Θ_D is ~ 200 K for $a\text{-Fe}_x\text{Zr}_{100-x}$,²² we might expect the data in Fig. 3 to follow straight lines with slopes β and $D^2=0$ intercepts $\gamma \equiv \lim_{T \rightarrow 0}(C_p/T)$. However, we can see immediately that while the data for the most Fe-rich ($x=39.0\%$) and Fe poor ($x=26.7\%$) samples do indeed follow the expected line, there are clear upturns in the other curves at the lowest temperatures ($T < 10$ K). The upturn becomes more marked as the Fe content increases from $x \sim 32\%$, reaches a maximum around $x=37\%$, and then dies away. We attribute the upturns to an electron mass enhancement arising from the presence of SF's. Similar, though generally weaker, upturns in $C_p(T)/T$ have been observed previously^{6-8,23,24} and also attributed to SF's.

The expression for $C_p(T)$ of an itinerant electron magnet in the presence of SF's is⁶

$$\frac{C_p(T)}{T} = \gamma + \beta T^2 + DT^2 \ln\left(\frac{T}{T_{\text{SF}}}\right), \quad T \ll T_{\text{SF}}, \quad (7)$$

where

$$\frac{\gamma}{\gamma_0} \equiv \frac{m^*}{m} = (1 + \lambda_{e-p} + \lambda_{\text{SF}}).$$

The first two terms of Eq. (7) are just the normal expression for a metal [Eq. (6)], except that γ now includes λ_{SF} , a mass enhancement term from SF's, in addition to the electron-phonon enhancement, λ_{e-p} . γ can still be identified as $\lim_{T \rightarrow 0}(C_p/T)$. The third term is negative and has a temperature dependence which is the signature of SF's. Fits of Eq. (7) to $C_p(T)$ of all our samples have been performed for $T < 5$ K. These are shown as solid lines in Fig. 3, where they give a good description of the data. Values of γ and D , derived from the fits,²⁵ are shown in Fig. 4, and both exhibit a clear peak at x_c , the critical concentration for ferromagnetism determined in the previous section, suggesting that the upturns in $C_p(T)/T$ are magnetic in origin.

Unfortunately, the second term of Eq. (7) and the denominator of the logarithm both contribute a T^3 term to $C_p(T)$.^{17,20} This normally makes a separate determination of β and T_{SF} impossible. However, we observed that at high temperatures (between 7 K and 10 K) all of our $C_p(T)$ data could be fitted by Eq. (6), which describes normal metallic behavior at temperatures $T < \Theta_D/20$ (up to about 10 K here²²). Neither the slope (β) nor the $T=0$ intercept (γ_{HT} , shown as open circles in Fig. 4) exhibits any structure around x_c . The absence of any change in the phonon contribution at the critical concentration of $\sim 37\%$ Fe^{17,20} eliminates the possibility that structural changes contribute to the upturns observed below 5 K. Furthermore, the high-temperature linear coefficient of $C_p(T)$, γ_{HT} , simply increases with x and is equal to γ for samples with $x < 32\%$ and $x = 39.0\%$. This smooth progression of γ_{HT} between the values of γ for the SF free alloys indicates that γ_{HT} arises from the electron-phonon effective mass enhancement λ_{e-p} without the effects of SF's (i.e., $\lambda_{\text{SF}}=0$) and that

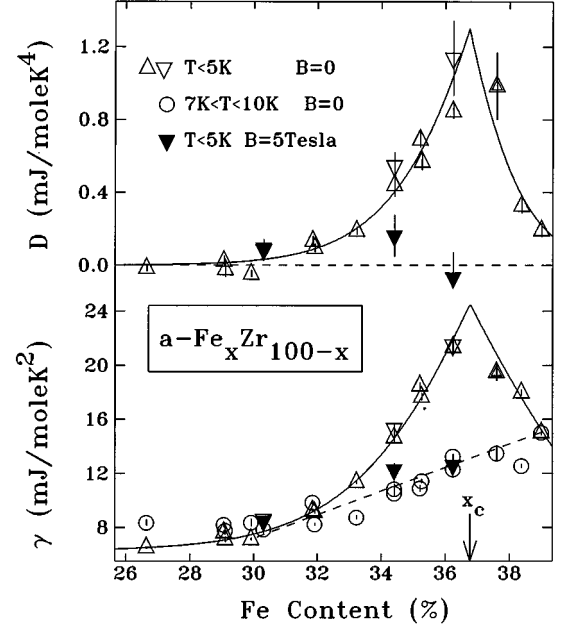


FIG. 4. SF parameters γ (Δ) and D (Δ) derived from fits of the zero-field data to Eq. (7). Also shown are values of γ_{HT} (\circ) from normal fits of Eq. (6) to $C_p(T)$ in the range $7\text{ K} < T < 10\text{ K}$. Downward-pointing triangles indicate magnetocalorimetry runs (Fig. 6) in zero field (open symbols) and in a 5 T field (solid symbols). The lines are guides to the eye.

the spin fluctuations are completely quenched by thermal effects as a result of the unusually low T_{SF} in this system (see below). The SF enhancement vanishes in a temperature range where the electronic contribution is still a significant fraction of the total $C_p(T)$, and the phonon term can still be represented by its low-temperature limiting form. In a system with a higher T_{SF} , the electronic heat capacity would only be a small fraction of the total at temperatures high enough for the SF enhancement to be zero, and higher-order contributions to the phonon term would greatly complicate the analysis. Given the good normal fits to the data in the temperature range $7\text{ K} < T < 10\text{ K}$, we believe that this is the first observation of the complete reduction of the effective electron mass m^* from its low-temperature, SF+phonon-enhanced value to its high-temperature, phonon-enhanced value.

With a reliable value for the phonon term β , we can now use Eq. (7) to obtain T_{SF} from the fitted values of D in Fig. 4. We find T_{SF} to be ~ 7 K, in broad agreement with earlier low-temperature resistivity results.^{12,13,17,20} Furthermore, assuming that the above interpretations of γ and γ_{HT} are correct, we can write

$$\begin{aligned} \gamma_{\text{HT}} &= \frac{1}{3} \pi^2 k_B^2 N_0(\varepsilon_F) (1 + \lambda_{e-p}) \\ &= \left(425 \frac{\text{mol K}^2}{\text{eV J atom}} \right)^{-1} N_0(\varepsilon_F) (1 + \lambda_{e-p}) \end{aligned} \quad (8)$$

and

$$\gamma = \left(425 \frac{\text{mol K}^2}{\text{eV J atom}} \right)^{-1} N_0(\varepsilon_F) (1 + \lambda_{e-p} + \lambda_{\text{SF}}). \quad (9)$$

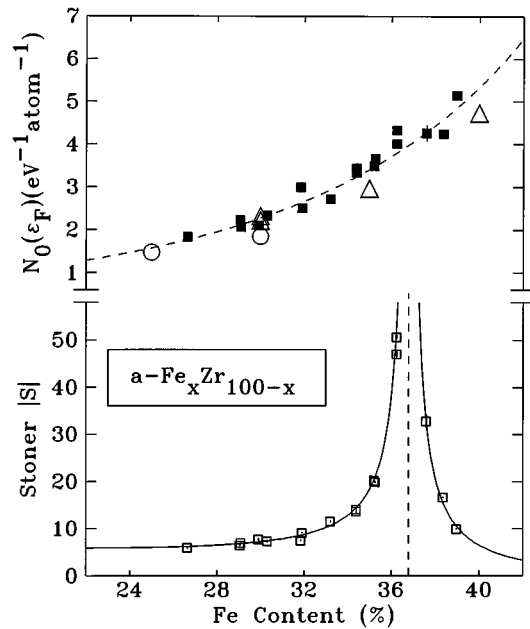


FIG. 5. Top: composition dependence of the bare density of states at the Fermi level $[N_0(\epsilon_F)]$ derived from γ_{HT} assuming a linear continuation of λ_{e-p} found in superconducting samples (Ref. 22). Data from Onn *et al.* (\circ) Ref. (22), Matsuura *et al.* (\triangle) (Ref. 26) and this work (\blacksquare). The dashed line is a guide to the eye. Bottom: $|S|$ vs x derived from γ_{HT} and $\chi(T=0)$ showing the divergence at $x=x_c$ where magnetic order develops.

Extrapolating estimates of $\lambda_{e-p}(x)$ determined from the McMillan relation in a previous study of superconducting compositions,²² we obtain values of $N_0(\epsilon_F)$ in agreement with previous work^{22,26} (Fig. 5). The excess which appears as the peak in γ at x_c in Fig. 4 is then attributed to λ_{SF} , which reaches a maximum value of ~ 1 at x_c (this should be compared with an extrapolated λ_{e-p} of ~ 0.4). Knowledge of $N_0(\epsilon_F)$ allows a determination of the Stoner enhancement factor S from Eq. (2). Taking χ from Eq. (3) and using $\mu_B^2 = 32.3 \text{ cm}^3 \mu\text{eV atom/mol}$, we obtain the values of $|S|$,²⁷ plotted in Fig. 5, which show the expected divergence at x_c .

We interpret the results presented above to mean that at very low iron concentrations $C_p(T)$ has no enhancement due to SF's ($\lambda_{SF}=D=0$), and $C_p(T)$ obeys the normal expression (6). As the Fe content is increased, we see the growing influence of SF's on the effective electron mass as an increase in D and γ (or λ_{SF}). These parameters reach a maximum at the critical concentration and then decrease with further increases in Fe content as the magnetism becomes firmly established and SF's less important. SF models predict that both γ and D should scale with the absolute value of the Stoner enhancement factor S , which also has its maximum at x_c (Fig. 5) and decreases as one moves away from the critical composition.⁶ This peaked composition dependence of γ , D , and S observed here is in accordance with SF models. Broadly similar results have been obtained for Ni_3Al alloys.^{6,7}

We emphasize here that the magnetic and calorimetric SF effects have been determined independently. S is derived from γ_{HT} , the high-temperature linear coefficient of

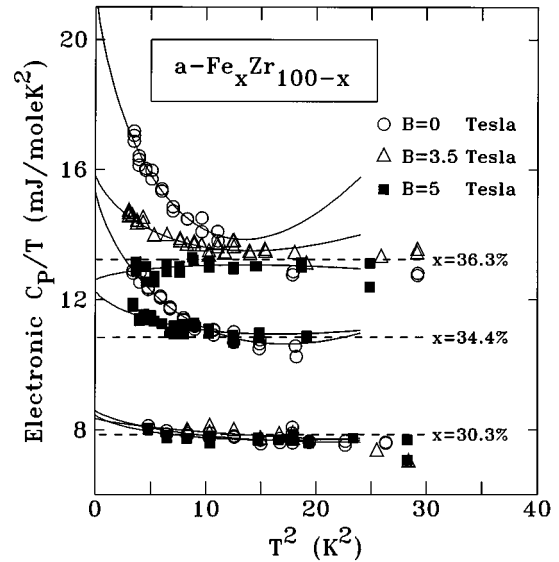


FIG. 6. Magnetic field dependence of the electronic $C_p(T)$ of three paramagnetic samples: $x = 30.3\%$, 34.4% , and 36.3% (estimated to have Stoner factors of 7, 14, and 50, respectively). The electronic $C_p(T)$ was determined by subtracting off the phonon contribution (βT^3), as discussed in the text. Solid lines are fits to Eq. (7) below 5 K. Dashed lines are values of γ_{HT} , the high-temperature linear coefficient of $C_p(T)$ measured in zero field. For clarity, some intermediate field curves have been removed.

the specific heat, which exhibits no structure at x_c , and χ from magnetization data, whereas the calorimetric signatures of SF come only from the low-temperature upturns which yield γ and D . The observation that γ , D , and S all rise to maxima right at $x_c \sim 37\%$, the critical concentration for ferromagnetism determined from magnetization measurements in the previous section, coupled with the absence of any features in either γ_{HT} or β at x_c , is strong evidence that the upturns in $C_p(T)/T$ are magnetic in origin. However, the critical test of our SF interpretation comes with the application of a magnetic field.

Figure 6 summarizes measurements of the electronic $C_p(T)$ for three paramagnetic $a\text{-Fe}_x\text{Zr}_{100-x}$ samples determined in various fixed magnetic fields between 0 and 5 T. The electronic $C_p(T)$ was obtained by subtracting off the βT^3 phonon contribution, where β was determined from fits to Eq. (6) for $7 \text{ K} < T < 10 \text{ K}$. The data are shown on the same axes with no offsets. The samples have Fe contents of $x = 30.3\%$, 34.4% , and 36.3% with Stoner factors, $S = 7$, 14, and 50, respectively. Note the rapid suppression of the upturn in the $x = 36.3\%$ case.

Many authors^{5,6} have warned that superparamagnetic clusters²⁸ may mimic SF effects in $C_p(T)$. Basic consideration of the magnetocalorimetry data for $x = 36.3\%$ in Fig. 6 allows us to rule out cluster explanations of the upturn. Statistical mechanics requires that increasing T and B should affect a superparamagnetic $C_{MAG}(T,B)$ in the opposite sense. However, plotting the data in Fig. 6 as $C_p(T)$ vs T shows that increasing the applied field or the temperature leads to a decrease in the excess specific heat for $x = 36.3\%$, in direct contradiction of cluster-based predictions. A more detailed discussion of this point has been presented elsewhere.^{17,20}

Fits of the SF expression (7) to $C_p(T)$ at all field values have been performed below 5 K, as before. Values of γ and D determined from magnetocalorimetry runs are plotted in Fig. 4 as solid symbols. The magnetocalorimetry results can be explained in terms of SF theory which expresses the change in $C_p(T)$ in an applied field as a change in the linear coefficient. $\gamma(B)$ is predicted to decrease in a field B as⁶

$$\frac{\gamma(B) - \gamma(B=0)}{\gamma(B=0)} = -0.1 \frac{S}{\ln S} \left(\frac{\mu_B B}{k_B T_{SF}} \right)^2. \quad (10)$$

The decrease in γ is referred to as the quenching of SF's and results from an energy gap, $\mu_B B$, which opens up in the SF quasidispersion curve and decreases the effect of SF's on the electronic $C_p(T)$. We can see immediately that Eq. (10) qualitatively explains the data in Fig. 6. For the $x=30.3\%$ sample, which shows no upturn in $C_p(T)/T$ at $B=0$, the application of fields up to 5 Tesla has no visible effect on $C_p(T)$. This is because $C_p(T)$ for this sample is not enhanced by SF's. The most nearly ferromagnetic sample, with $x=36.3\%$, shows the biggest upturn at $B=0$ of any of our samples. The application of a 5 T field, however, completely removes the upturn in the electronic $C_p(T)/T$. Both the large upturn and the large quench rate result from the high Stoner factor $S \sim 50$. Furthermore, in the 5 T field, the electronic $C_p(T)$ is reduced to γ_{HT} , i.e., the continuation of the high-temperature $B=0$ behavior extrapolated to lower temperatures. This indicates that, through the application of a 5 T field, we have observed, the complete quenching of SF's. The intermediate sample provides a final confirmation of the SF model. Given its weaker upturn, one might initially expect that a field would suppress the SF contribution more rapidly, but quite the opposite is observed. The upturn is reduced, but certainly not eliminated, in 5 T and $C_p(T)/T$ (in 5 T) is still larger than γ_{HT} . This is because both the amplitude of the upturn and the quenching rate in a field are controlled by S , which is only ~ 14 in the $x=34.4\%$ sample. Because of the lower value of S for $x=34.4\%$, both the upturn and the quench rate are reduced, as predicted by the theory [Eqs. (7) and (10)].

Using Eq. (10), $T_{SF} = 7$ K, and $\mu_B/k_B = 0.672$ K/T, together with the values of S determined from the susceptibility and γ_{HT} measured in zero field, we have determined the expected quench rates. These are given in Table I, together with the experimental quench rates $d[\gamma(B)/\gamma(B=0)]/d[B^2]$. The approximate agreement between the measured and independently predicted quench rates is our strongest quantitative evidence that the upturns in the electronic $C_p(T)/T$ arise from SF's. The field dependence of the electronic $C_p(T)/T$ data for $x=36.3\%$ is a clear observation of the complete quenching of SF's by a

TABLE I. Comparison of theoretical and experimental quench rates $d[\gamma(B)/\gamma(B=0)]/d[B^2]$ (in $\%/T^2$). The theoretical quench rates have been determined using Eq. (10), estimates of the Stoner factor, S , and $T_{SF} = 7$ K. The experimental quench rates were determined from linear fits of $\gamma(B)$ [from Eq. (7)], vs B^2 .

$a\text{-Fe}_x\text{Zr}_{100-x}$ x	Stoner factor S	Theoretical quench rate $\%/T^2$	Measured quench rate $\%/T^2$
30.3	7	-0.33	-0.07
34.4	14	-0.49	-0.80
36.3	50	-1.2	-1.5

magnetic field. These data, coupled with the observation of only partial quenching in $x=34.4\%$ under similar conditions, are the most convincing calorimetric evidence to date for the presence of SF's in any metal.

IV. CONCLUSIONS

The ground-state susceptibilities of the five paramagnetic $a\text{-Fe}_x\text{Zr}_{100-x}$ samples are consistent with the exchange-enhanced susceptibilities of near ferromagnets with a critical concentration of $x_c \sim 37\%$. At high temperatures, the susceptibility is reduced, following a Curie-Weiss law with $\Theta_{CW} < 0$. This is consistent with the reduction of $\chi(T)$ by thermally activated spin fluctuations.

The absence of structural variations, coupled with the conveniently low T_{SF} , makes $a\text{-Fe}_x\text{Zr}_{100-x}$ the cleanest system in which to study spin fluctuations. Measurements of the low-temperature $C_p(T)$ in $a\text{-Fe}_x\text{Zr}_{100-x}$ show an enhancement of the effective electron mass at low temperatures which is consistent with that predicted for SF's. We have also reported the first observation of the complete quenching or suppression of SF modes both by high magnetic fields and at elevated temperatures, providing the clearest evidence to date of SF's in the electronic properties.

ACKNOWLEDGMENTS

This work was supported by grants from the Graduate Faculty of McGill University, the Walter C. Sumner Foundation, Nova Scotia, the Natural Sciences and Engineering Research Council of Canada, and Fonds pour la formation de chercheurs et l'aide à la recherche, Québec. We would like to thank Z. Altounian who provided some of the samples studied here, and assisted with many aspects of their characterization. All of us have benefited greatly from the many helpful discussions with J.O. Ström-Olsen over the course of this work.

¹T. Moriya, *Spin Fluctuations in Itinerant-Electron Magnetism* Vol. 56 (Springer-Verlag, Berlin, 1985).

²P. Mohn and E. P. Wohlfarth, *J. Phys. F* **17**, 2421 (1987).

³G. G. Lonzarich and L. Taillefer, *J. Phys. C* **18**, 1 (1985).

⁴G. G. Lonzarich, *J. Magn. Magn. Mater.* **54-57**, 612 (1986).

⁵E. P. Wohlfarth, in *Proceedings of International Conference on*

Itinerant Electron Magnetism, 1976, edited by R. D. Lowde and E. P. Wohlfarth (North-Holland, Amsterdam, 1977), p. 305.

⁶K. Ikeda, S. K. Dhar, M. Yoshizawa, and K. A. Gschneidner, Jr., *J. Magn. Magn. Mater.* **100**, 292 (1991).

⁷S. K. Dhar, K. A. Gschneidner, Jr., L. L. Miller, and D. C. Johnston, *Phys. Rev. B* **40**, 11 488 (1989).

- ⁸G. R. Stewart, J. L. Smith, A. L. Giorgi, and Z. Fisk, *Phys. Rev. B* **25**, 5907 (1982).
- ⁹N. R. Bernhoeft, G. G. Lonzarich, P. W. Mitchell, and D. McK. Paul, *Phys. Rev. B* **28**, 422 (1983).
- ¹⁰E. Batalla, Z. Altounian, and J. O. Ström-Olsen, *Phys. Rev. B* **31**, 577 (1985).
- ¹¹M. Trudeau, R. W. Cochrane, D. V. Baxter, J. O. Ström-Olsen, and W. B. Muir, *Phys. Rev. B* **37**, 4499 (1988).
- ¹²J. Ström-Olsen, Z. Altounian, R. W. Cochrane, and A. B. Kaiser, *Phys. Rev. B* **31**, 6116 (1985).
- ¹³Z. Altounian, S. V. Dantu, and M. Dikeakos, *Phys. Rev. B* **49**, 8621 (1994).
- ¹⁴E. C. Stoner, *Proc. R. Soc. London A* **165**, 372 (1938).
- ¹⁵D. M. Edwards and E. P. Wohlfarth, *Proc. R. Soc. London A* **303**, 127 (1968).
- ¹⁶F. R. de Boer, C. J. Schinkel, J. Biesterbos, and S. Proost, *J. Appl. Phys.* **40**, 1049 (1969).
- ¹⁷A. LeR. Dawson, Ph.D. Thesis, McGill University, Montréal, 1994.
- ¹⁸P. Mohn, D. Wagner, and E. P. Wohlfarth, *J. Phys. F* **17**, L13 (1986).
- ¹⁹L. Taillefer, Ph.D. Thesis, Jesus College, Cambridge, 1986.
- ²⁰A. LeR. Dawson and D. H. Ryan, *J. Appl. Phys.* **75**, 6837 (1994).
- ²¹D. L. Martin, *Phys. Rev. B* **8**, 5857 (1973).
- ²²D. G. Onn, L. Q. Wang, Y. Obi, and K. Fukamichi, *J. Non-Cryst. Solids* **61**, 1149 (1984).
- ²³R. J. Trainer, M. B. Brodsky, and H. V. Culbert, *Phys. Rev. Lett.* **34**, 1019 (1975).
- ²⁴K. Ikeda and K. A. Gschneidner, Jr., *Phys. Rev. Lett.* **45**, 1341 (1980).
- ²⁵The parameters for the $x=37.6\%$ sample were derived using a modified function, since this sample showed an ordering transition at about 4 K. Entropy measured under the transition spike gave an estimate of $\sim 0.02\mu_B$ for the ordered moment of the $x=37.6\%$ sample (Ref. 17).
- ²⁶M. Matsuura, U. Mizutani, and K. Fukamichi, in *Proceedings of the Fifth International Conference on Rapidly Quenched Metals*, Würzburg, Germany, edited by S. Steeb and H. Warlimont (North-Holland, Amsterdam, 1984), Vol. 1, p. 1019.
- ²⁷ S is related to \bar{T} through $S \equiv (1 - \bar{T})^{-1}$, and \bar{T} passes through one at $x=x_c$, causing S to change sign. Thus $|S|$ is well defined even in an ordered system; however, it is not, strictly speaking, a Stoner enhancement factor in such cases.
- ²⁸R. L. Falge, Jr. and N. M. Wolcott, *J. Low Temp. Phys.* **5**, 617 (1971).